Monte Carlo analysis of the energy deposition process in the boron neutron capture therapy

M. H. Hassan
Nuclear Eng., Dept., Alexandria University, Alexandria, Egypt

One of the promising features of Egypt's Second Research Reactor, ETRR-2, is the Boron Neutron Capture Therapy (BNCT) facility. In BNCT, The total absorbed doses resulting from neutron irradiation is mainly the sum of the absorbed doses from the $^{1}H(n,\gamma)^{2}H$, $^{14}N(n,p)^{14}C$ and the $^{10}B(n,\alpha)^{7}Li$ reactions in the cells and medium There was a need to develop a consistent set of raw dosimetric data to be used in the calculations rather than approximate ranges and energy deposition rates in tissue as it is always found in the literature. There was also a need to compare doses delivered at different boron concentrations. Helium, lithium, and proton irradiation with their proper branching ratios were simulated for brain, skull, water, as well as polyethylene phantoms for boron concentration from 20 to 60 μ g/g. Energy deposition rate dE/dX in the different phantom media are presented as well as curve fittings for its value in brain. It was concluded that simulation of energy deposition in both brain and skull tissues can use the same values for energy deposition rate for alpha and lithium ions. Water phantoms tend to overestimate the energy deposition rates of Li ions, and to a lesser degree, alpha ions compared with the brain tissues. Regardless of the fact that the range of the carbon ions in brain tissue is of the order of 0.5 micron, their rate of energy deposition is relatively high. The question remains whether this rate of energy deposition can be neglected from a radiobiological point of view or not.

من أهم وحدات مفاعل مصر البحثي الثاني وحدة العلاج باستخدام طريقة أسر البور ون للنيوترونات. في تلك الطريقة، تنشأ الجرعة الإشعاعية العلاجية الكلية من تجميع الجرعات الناشئة من التفاعلات $^{1}H(n,\gamma)^{2}H$, $^{14}N(n,p)^{14}C$ علاوة على $^{10}B(n,\alpha)^{7}Li$ في الخلايا والوسط المحيط هذا. كان هناك حاجة لتطوير مجموعة متناسقة من بيانات الجرعات لاستخدامها في الحسابات بدلا من الاعتماد على مدى الجسيمات في الماء والمستخدم عادة أو بدلا من الاعتماد على الطرق التقريبية لامتصاص الطاقة في الخلايا الحية والتي عادة ما كان يتم استخدامها من قبل. تمت محاكاة تشعيع تركيبات الفانتوم المختلفة: ما يماثل خلايا المخ، عظام الجمجمة، الماء، والبولي ايثيلين وذلك بواسطة جسيمات ألفا، ليثيوم، وبروتونات مع الأخذ في الاعتبار نسب طاقاتها المختلفة. تم اعتبار أن تركيب الخلايا السرطانية يماثل خلايا المخ. تركيز البور ون تراوح بين ٢٠ إلى ٦٠ ميكروجرام لكل جرام من الخلايا. تم تطوير معادلات لوصف المنحنيات التي تم الحصول عليها والتي تمثل معدل امتصاص الطاقة dE/dX فى المادة للفانتوم المختلفة. أثبتت طريقة المحاكاة بالمونت كارلو أنها أداة قوية للتنبأ بالجرعات نتيجة لتركيزات مختلفة للبورون. بينت النتائج أنه يمكن استخدام نفس معدلات امتصاص الطاقة لجسيمات ألفا والليثيوم وذلك عند محاكاة التأثير في المخ أو عظام الجمجمة على حد سواء. معدلات امتصاص الطاقة في الماء تميل إلي التنبؤ بمعدلات عالية لامتصاص الطاقة خاصة بالنسبة لجسيمات الليثيوم. رغما عن أن مدي أيونات الكربون في خلايا المخ يبلغ نصف ميكرون فإن معدل امتصاص الطاقة عالي جدا. يبقي السؤال من الناحية البيولوجية عما إذا كان من الممكن إهمال هذا المعدل من الامتصاص كما هو متبع أم لا .

Keywords: Boron neutron capture therapy, Microdosimetry, Rate of energy deposition, Transition zone dosimetry.

1. Introduction

One of the promising features of Egypt's Training Research Reactor-2, ETRR-2, is the Boron Neutron Capture Therapy (BNCT) facility. It will be the first in Africa and it may target a population of 600 million people where it is almost certain that cancer and its management will constitute a major health problem by the year 2000 and beyond [1].

Alexandria Engineering Journal. Vol. 40 (2001), No. 2, 169-180

BNCT is still in its early stages of clinical development regardless of the initiation of the method several years ago. In 1932, a biophysicist, G. L. Locher of the Franklin Institute at Pennsylvania introduced the concept of neutron capture therapy (NCT) [2]. First clinical trials of BNCT were started in Boston, USA, by Prof. W. Sweet between 1951 and 1961. A Japanese neurosurgeon H. Hatanaka modified the technique, and treated his first patients in 1968. Patient trial started 1992 in the USA [3]. In 1997, A Japanese group has treated more than 160 brain tumor patients by BNCT [2].

There are three components necessary for the success of BNCT: (1) A nontoxic boron compound, (2) Selective assimilation of the boron compound into the tumorous cells, and (3) activation of the boron compound by neutrons with an energy adequate for penetration to the depth of the tumor [4]. Each boron-neutron interaction produces an alpha particle and a lithium ion according to the reaction B(n,α)Li. These highly-energetic charged particles deposit their energy within a geometric volume that is comparable to the size of a malignant cell, leading to a high probability of cell inactivation by direct DNA damage [4]. Alpha particles, for example, has a path length of approximately 8 microns [2], and an average Linear Energy Transfer (LET) of 200 keV/μ [5]. The success of BNCT depends; among other things; on Boron content in tumor and normal tissues [5]. An essential feature of any clinical treatment planning procedure should be the capability of prospectively and retrospectively evaluating radiation doses to skull and scalp tissues [6].

2. Clinical considerations

Some of the medical requirements for the irradiation field in BNCT are [7]:

(1) Total of the doses from the B(n,α)Li and neutron and gamma-ray reaction in tissue should be above 20 Gy (i.e., 2000 rad) in the affected part. This is for 30 μ g boron per gram of tissue, which is the regularly used boron concentration.

(2) Total of the doses from the B(n,α)Li and neutron and gamma-ray reaction in any part of the body should be below 50 Gy. This is for a 10 μg of boron per gram of healthy tissue which is the assumed boron concentration in healthy tissue.

(3) The ratio of B(n, α)Li reaction dose to neutron and gamma-ray dose should be high.

3. Dosimetry analysis

The sequence of steps for dosimetry analysis [9] starts with the development of "raw" dosimetric data by Monte Carlo simulation and ending with the calibration of Monte Carlo derived treatment plans by experimental mixed-field dosimetry. Raw dosimetric data means energy deposition rates, particle ranges, etc., i.e., the specific data needed to complete a realistic Monte Carlo simulation.

In BNCT, The total absorbed doses resulting from thermal neutron irradiation is the sum of the absorbed doses mainly from the $^{1}H(n,\gamma)^{2}H$, $^{14}N(n,p)^{14}C$ and the $^{10}B(n,\alpha)^{7}Li$ reactions in the cells and medium and from the primary gamma-rays [10]. The localized dose effect is based mainly on protons, alpha particles, and the ^{7}Li nuclei [11]. The Carbon atoms are usually neglected since their energy is 0.04 MeV and their range in water is 0.02 μm (range of the other particles in water ranges from 4.8 to 10.8 μm) [11].

3.1. Phantoms and involved reactions

The most commonly used brain and skull compositions are given in table 1 below [9]. Cancer cells are taken to be of the same composition as the normal brain cells.

Table 1
Commonly used brain and skull compositions [9]

Element	Brain		Skull	
	W%	Atomic %	W%	Atomic %
H	10.6	65.2	5	49.3
C	14	7	14	11.5
N	1.84	0.8	4	2.8
O	72.6	27	45	27.7
P	0	0	21	3.5
Ca	0	0	11	5.2

Other related brain and skull properties as well as cell dimensions are given below:

Table 2
Atomic composition of water, water plus nitrogen, and polyethylene phantoms

Element	Water [13]	ater + Nitrogen [16]	olyethylene [15]
H	6.67 (11.11 W%)	6.19 (10.9 W%)	6.67 (14.29 W%)
O	3.33 (88.89 W%)	3.02 (87.23 W%)	--
N	--	.8 (1.84 W%)	--
C	--	--	3.33 (85.71 W%)

Elemental composition of brain tissue: $(C_5H_{40}O_{18}N)_n$ [11], Density of brain: 1.047×10^3 kg/m^3 [9], Density of skull: 1.5×10^3 kg/m^3 [9], Cell radii: 5 μm [12], Cell nuclear radii: 2.5 μm [12]. Also, a regularly used composition of the body phantom is water only (11.11 wt% H and 88.88 wt% O, density = 1.0×10^3 kg/m^3) [13]. Sometimes, a phantom filled with water containing 1.84 W% nitrogen is used [13,14]. Finally, a polyethylene phantoms (density 0.91×10^3 kg/m^3) is sometimes used for dosimetric measurements [15]. These phantom compositions are given in table 2.

It is worth noting that regardless of the fact that the capture cross sections of neutrons in nitrogen and hydrogen atoms are small, abundant quantities of N and H exist in normal tissues; as indicated above. Thus, the upper limit of the neutron fluence that can be delivered is determined by the tolerance of the surrounding normal tissues to protons and gamma rays produced by these capture reactions [5]. This is explained below when the involved cross sections as well as element concentrations are taken into considerations. Finally, we have to note that we must accumulate at least 20 micrograms of ^{10}B per gram (equivalent to 20 ppm) of tumor in the cancer cell [7].

The $^{10}B(n,\alpha)^7Li$ reaction details are as follows [12]: Reaction cross section: 3837 b, Energy released in reaction: 2.79 MeV, branching ratios are as follows: 6.3% (alpha energy: 1.78 MeV, Li energy: 1.01 MeV) and 93.7% (alpha energy: 1.47 MeV, Li energy: 0.84 MeV), Average interactions per cubic micrometer in unit density tissue (For a neutron fluence of 10^{13} neutrons/cm^2 and a uniform boron concentration of 20 μg/g) is 0.0462.

The $^{14}N(n,p)^{14}C$ reaction details are as follows [12]: Reaction cross section: 1.81 b, Energy released in reaction: 0.63 MeV, Proton's energy: 0.59 MeV, Recoil carbon energy: 40 KeV, Average interactions per cubic micrometer in unit density tissue (For a neutron fluence of 10^{13} neutrons/cm^2 and a uniform nitrogen concentration of 3.5 %): 0.0273.

3.2. Calculation of the relative biological effectiveness (RBE)

In order to develop objective treatment planning criteria for BNCT, it is necessary to estimate the different RBE factors for the various radiation components comprising the dose field [17]. Dosimetry is made complicated by the fact that there are different radiation dose components that need to be measured simultaneously and separately [15]. The mixed radiation field presents a unique problem in treatment planning in BNCT. The RBE's of the different components are not only different, they also change with depth in tissue (resulting from energy changes), as does the overall mix of high and low Linear Energy Transfer (LET) radiation [18]. It is worth noting that to be successful, the dose delivered by boron must have a certain minimum value compared to the other dose contributions in the treatment volume [19].

Depending on the different simplifying assumptions, the RBE's determined by different methods may vary considerably [18]. An RBE value of 1.0 was assumed for all gamma rays, 1.6 for fast neutrons and protons, and 2.3 for the Boron fission reaction [20]. RBE factors of up to 7 have been measured for melanoma cells exposed to melanim precursors labeled with ^{10}B [17].

For the response of the microvasculature to ^{10}B dose, RBE factors of 2-3 have often been assumed [17]. RBE values assigned to the alpha particles have ranged from 1.94-6.01 depending on the biologic system [5].

3.3. Transition zone dosimetry

In many situations, irradiated material or tissue is homogenous and boundary effects do not contribute significantly to the radiobiological action. This is the case if the object is large compared with the range of the ionizing particles and its composition is uniform over distances which are much less than the particle range [21]. However, there are circumstances-for example, at the surface of the body or in an organ as heterogeneous as bone-where more sophisticated methods of dosimetry are required. The distribution of absorbed dose near an interface between two dissimilar materials, that is, in a transition zone, has been considered. This is related to dose distributions over distances which are less than the range of the ionizing particles, and frequently, therefore, over distances of a few microns or a few hundred microns near the boundary of two dissimilar materials.

It is also worth noting that KERMA and absorbed doses are practically equivalent only under conditions of secondary charged-particle equilibrium [22] like in an extended medium irradiated by fast neutrons, except very close to an interface and except very close to a source of neutrons such as a needle containing ^{252}Cf. Similar effects occur near the surface of bone for cell irradiation in vitro. Very close to the surface, where the secondary charged particles are not in equilibrium, the ionization is more dense and has a higher RBE.

In the BNCT ions fluxes depend upon the concentration of nitrogen and boron and the distributions of these isotopes in or near the cell [12]. These concentrations are usually not uniform [17]. Thus, the calculation of dose to the nucleus from ions generated in the nitrogen and boron presents the same problem as the 'transition zone dosimetry' [12]. Here the ranges of the three of the ions (p,α,Li) are similar to typical cell diameters, and since the concentrations of the nitrogen and boron are not uniform, then important deviations from the equilibrium doses are expected [12].

Kitao [23] indicated that the low energy charged particles not only have very short range but also their specific ionization decreases rapidly with their traveling path in matters such as tissue. That is, the Bragg peak does not appear in the curve of the specific ionization. This implies that the assumption of a constant energy loss (or energy transfer) in such matter, often used in the dose calculation for the long-range alpha particles, is a rather poor approximation.

3.4. Previous microdosimetry analysis relevant to the BNCT

Davis et al. [16] while determining the relative biological effectiveness of the $^{10}B(n,\alpha)^{7}Li$ reaction in HeLa cells, used the LET vs. distance in tissue for the 1.5 MeV alpha rays from the experimental work of Rotondi. The use of this data gives the alpha particle a range of 7 microns in tissue. The ^{7}Li values are calculated from the theoretical estimates given by Northcliffe in which a ^{7}Li particle of 0.8 Mev energy has a range of 3.5 microns in tissue.

Kitao [23] has used analytical methods to calculate dose to the nucleus using approximate LETs for the ions. He used the energy loss values for the helium and lithium particles in water. He treated only the (n,α) reaction in boron neglecting the neutron capture reactions in nitrogen. Kitao [23] also indicated that detailed experimental or theoretical knowledge of stopping power or specific energy transfer for tissue by alpha and lithium particles from the B(n,α)Li reaction is required.

Kobayashi and Kanda [24], using approximate LETs for the ions, calculated analytically the absorbed dose in a cell nucleus when boron is injected into the cytoplasm. In the calculations, the range-LET relation of heavy charged particles in tissue is approximated by a definite linear equation, LET = a Y + b, according to Kellerer's approximation of tracks and was

calculated from the tabulated data of Northcliffe and Schilling for water. They found out that the cell nucleus is more damaged when particles produced inside the nucleus lose more energy at the initial part of their range and when particles produced outside the nucleus lose more energy at the last part of their range, which clearly indicate that the shape of the range-LET curve has a great impact on BNCT dosimetry.

Gabel et al. [25] used a simple integral equation which was fitted to the data of Northcliffe and Schilling in water. For the ^{7}Li and ^{4}He particle, the equations were:

$$dE_{Li}/dR = 92.232\ R - 7.1009\ R^2$$
$$dE_{He}/dR = -4.05\ (R-1.36)^2 + 234.0$$

Here R is the residual range of the particle in question, and dE/dR is the energy dissipation (in keV/μm). The maximum values for R are 4.81 and 8.96 μm, for the ^{7}Li and the ^{4}He ions respectively. The above equations give total deposited energies of 804 and 1500 keV, respectively, which should be compared to the values of 852 and 1492 keV given by Northcliffe and Schilling. It is important to note that Gabel et al. [25], while calculating the BNCT dose, estimated the nitrogen contribution from the formulae of Kitao, which is valid only for alphas and lithium ions rather than the lower-LET protons.

Fukuda et al. [26] also calculated BNCT doses. They estimated the nitrogen contribution from the formulae of Kitao, which, as indicated before, is valid only for alphas and lithium ions rather than the lower-LET protons.

Charlton [12] calculated average dose and dose distribution in cell nuclei from ions produced by thermal neutron nuclear reactions in nitrogen and ^{10}B. He discussed the effect of interface on dose distribution and indicated that all previous approaches have assumed that the ionizing particles traveled in straight paths with stopping powers or LETs given by simple mathematical function. In his work, protons and alpha stopping powers were taken from ICRU Report 36. Stopping powers for lithium ions were taken from Northcliffe and Schilling for water. The proton range calculated from this method is 10.5 μm, the two alpha particles have ranges 9.2 and 7.5 μm and the two lithium ions have ranges of 9.5 and 5.2 μm.

4. Need for this work

It is obvious from the previous literature survey that ranges of alpha, lithium, and proton particles were taken from different references and for different media, namely, water and tissue with the result of dealing with inconsistent values from different sources. Thus, there is a need for a consistent set of raw dosimetric data in brain tissue for the different particles. Detailed energy deposition vs. distance due to the transport of these particles in brain tissue is also needed for the proper estimation of RBE values. Also, there is a need to evaluate the impact of brain vs. skull tissue on the ranges and energy deposition of the different particles for the proper evaluation of the BNCT treatment in brain. Other regularly head-phantom materials like water and polyethylene need also to be considered to have a consistent set of data for the different head phantoms. Finally, analytic expressions for the energy deposition vs. distance in the different media is needed for the proper microdosimetry simulations. All of the above analysis needs to be evaluated for the different boron concentrations used in the BNCT to be able to assess the effect of different clinical cases.

5. Calculations

The TAMIX code [27] was used for the Monte Carlo simulation of the energy deposition process in the BNCT. The usual practice in dosimetry analysis of the BNCT to assume the following [23]:

(1) The boron atoms are distributed uniformly in the boron-containing medium.

(2) The alpha particle and the recoil lithium nucleus are emitted isotropically and in opposite directions. Thus, it was regarded that the energy absorbed at any point is delivered by the alpha particle and the recoil

lithium nucleus [23], regardless of the fact that they are emitted from different boron nuclei.

The program is used to calculate energy deposition of various kinds of particles, which are a more useful guide to cell survival than average dose [12]. The simulation includes the alpha and lithium ions from the boron fissioning and the protons emitted from the $^{14}N(n,p)^{14}C$ reaction. Proper branching ratios were simulated as indicated below. In the nitrogen neutron capture reaction, the 40 KeV recoil carbon ions were neglected. Respective ion energies are as follows: α energy (93.7%): 1.47 MeV, Li energy (6.3%): 1.78 MeV, Li energy (93.7%): 0.84 MeV, Li energy (6.3%): 1.01 MeV, ^{1}H energy: 0.59 MeV.

Simulations were carried out for brain and skull tissues as well as water and polyethylene phantoms. These target compositions are given in tables 1, and 2

5.1. Analysis of the rate of energy deposition in the BNCT

Energy deposition due to Nitrogen thermal Neutron Capture (NNC), i.e. due to protons, as well as that due to the BNCT (i.e., due to alpha and lithium ions) in brain tissues were compared. Energy deposition consists of both electronic and nuclear energy depositions. As expected nearly all of the energy deposition is of the electronic type with small portion of nuclear energy deposition by end of the particle track.

The rate of energy deposition due to BNCT was analyzed by considering the rate of energy deposition in the different phantoms. Comparison was made between energy deposition of lithium and alpha particles as well as protons in an infinitesimal volume of a brain cell. This is done to be able to roughly compare the BNCT dose to the NNC dose. Relative values were calculated by considering the proper reaction rates in the infinitesimal volume. This was done by taking into considerations the absorption cross sections of boron (3837 b) and nitrogen (1.81 b) for thermal neutrons. Then the different boron and nitrogen concentrations in the brain cell were considered. Nitrogen concentrations of 0.8 atomic % in brain tissues were considered. Boron concentrations of 20 to 60 μg/g (i.e., 20 to 60 ppm [7]) in brain tumour tissue were considered also. This is done by multiplying dE/dX by $(N_B \times \sigma_{a\text{-}B}) / (N_{Ni} \times \sigma_{a\text{-}Ni})$. Thus, the ratio between rate of energy deposition dE/dX of He and Li particles divided by the dE/dX due to protons, were multiplied by 5.3, 7.95, 10.6, 13.25, and 15.9 respectively for the 20 to 60 μg/g boron doses, which was indicated before to be the regularly used boron concentrations. As expected, it was assumed that both boron and nitrogen nuclides are exposed to the same neutron flux. Relative values of dE/dX were compared with those resulting from boron concentration in normal brain tissue of 10 ppm which is assumed for a boron concentration of 30 ppm in brain tumor tissue [7].

6. Results and discussions

6.1. Rate of energy deposition

Rate of energy deposition, in keV/μm for the different particles are shown in Figs. (1-4) for brain, skull, water, polyethylene phantoms. table 3 shows a comparison of the numerical values for the respective ranges.

Table 3
Ranges for helium, lithium, and protons in different phantoms used

	Range in different media		
	Helium	Lithium	Proton
Water	10.8 ± 0.4	5.9 ± 0.3	10.2 ± 0.2
Brain	8.2 ± 0.5	3.8 ± 0.2	10.2 ± 0.2
Skull	8.1 ± 0.5	3.7 ± 0.2	10.1 ± 0.3
Polyethylene	7.7 ± 0.5	3.5 ± 0.2	10.3 ± 0.2

From table 3, we conclude:
(1) Ranges of alpha and lithium ions in brain and skull are nearly the same. Simulation of energy deposition in both tissues (brain and skull) can use the same values for energy deposition rate.
(2) The use of rate of energy deposition values for water tend to overestimate the ranges of

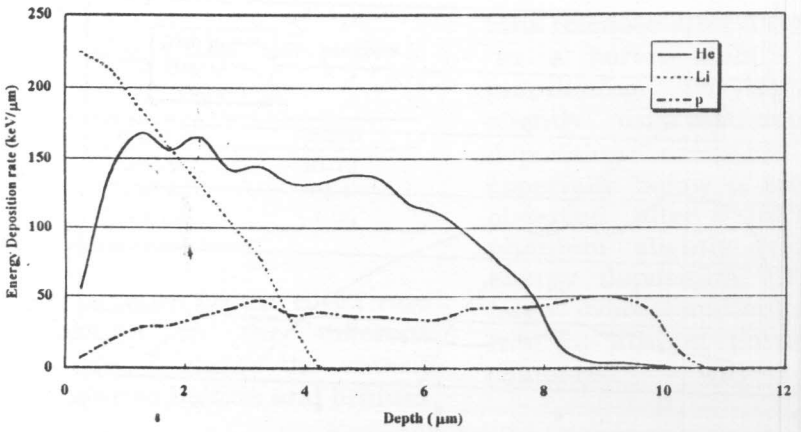

Fig. 1. Rate of energy deposition (keV/μm) in brain tissues.

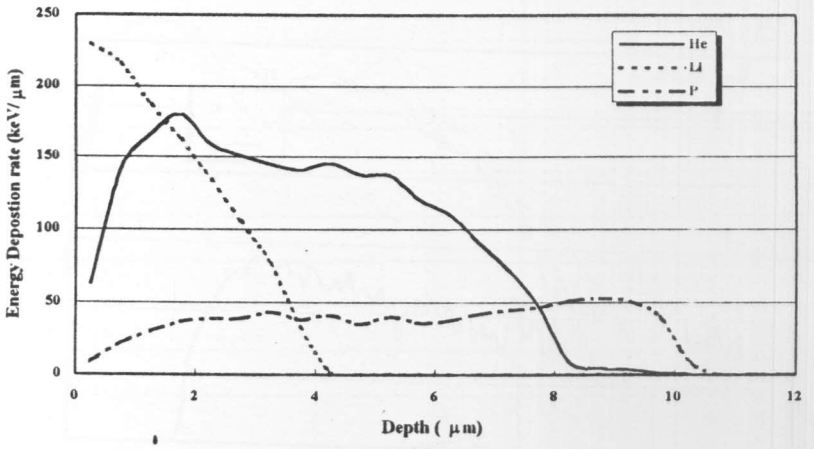

Fig. 2. Rate of energy deposition (keV/μm) in skull tissues.

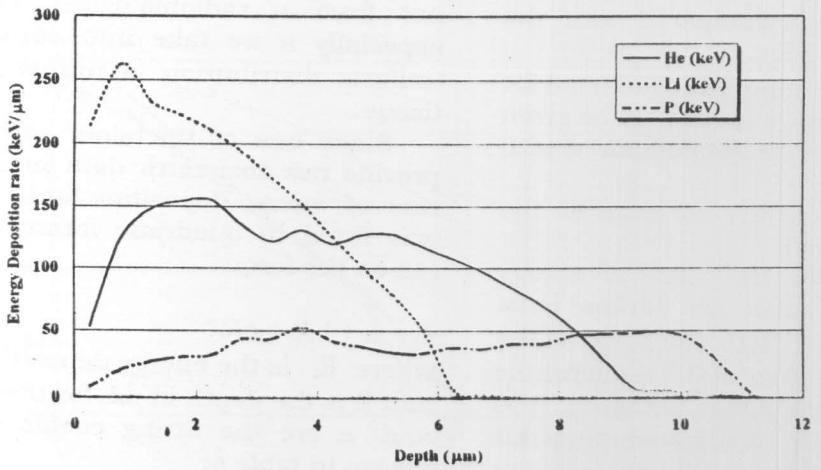

Fig. 3. Rate of energy deposition (keV/μm) in water.

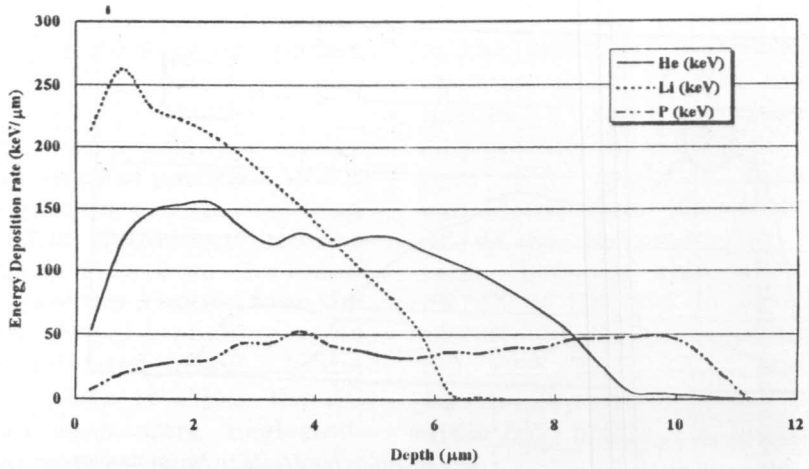

Fig. 4. Rate of energy deposition (keV/μm) in polyethylene.

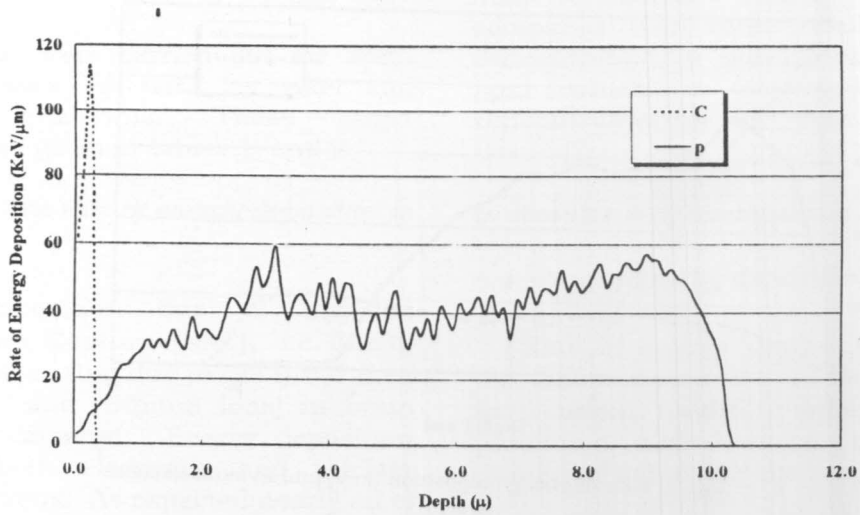

Fig. 5. Rate of energy deposition in brain tissues for C ions. Rate of energy deposition for protons is shown for comparison.

alpha and lithium ions compared with the brain tissues.

(3) When polyethylene phantoms are used for BNCT dose estimations, care should be given to the rather small ion ranges compared with actual brain tissues.

(4) Proton ranges are nearly the same for the different phantoms used.

Finally, fig. 5 shows the rate of energy deposition in brain tissue for carbon ions. Regardless of the fact that the range of the carbon ions is of the order of 0.5 a micronthe rate of energy deposition exceeds 100 keV/μm. The question remains whether this rate of energy deposition can be neglected or not from a radiobiological point of view, especially if we take into consideration the uniform distribution of nitrogen in the brain tissue.

Since one of the aims of this work is to provide raw dosimetric data for the BNCT, the rate of energy deposition for the brain tissue was fitted to quadratic formulae for the ith ion on the form:

$$E_i = a + bR_i + cR_i^2$$

where E_i is the energy deposition in keV/μm and R is the depth in μm for the ith ion.. a, b, and c are the fitting coefficients. This is shown in table 4.

Table 4
Fitting coefficients for helium, lithium, and protons in brain tissues

	Helium	Lithium	Proton
Brain	114.05*	243.93	10.12
	19.47	-48.62	12.1
	-3.33	-1.22	-1.06

* Numbers refer to a, b, and c respectively.

Finally, to properly account for the BNCT rate of energy deposition in the different phantoms, figs. 6 and 7 shows the rate of energy deposition due to helium and lithium ions released after a thermal neutron capture in a boron atom. Two points are worth mentioning. For alpha ions, water phantom slightly underestimates the rate of energy deposition compared with brain phantoms especially below 6 microns. The reverse is observed after 6 microns where the water phantom slightly overestimates the rate of energy deposition. The other point is the large overestimation of the energy deposition rate for lithium particles in water phantoms compared with brain phantoms.

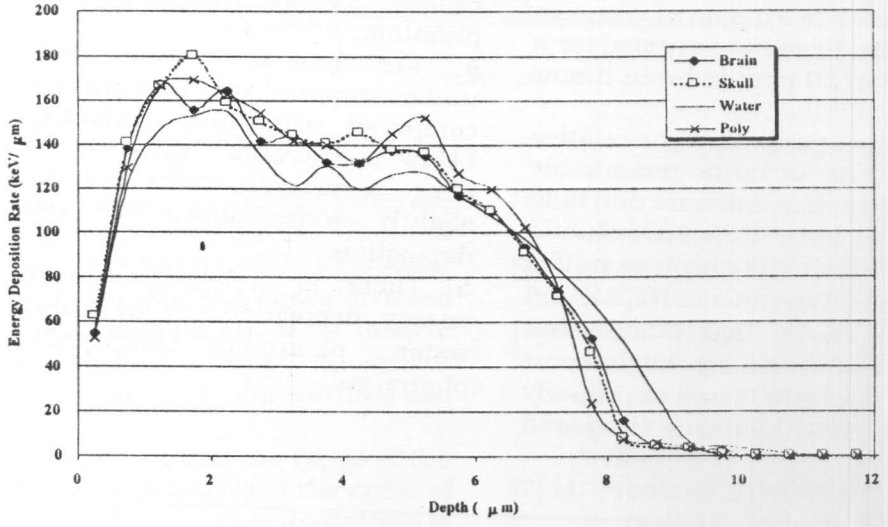

Fig. 6. Rate of energy deposition in different tissues due to helium ions (keV/μm).

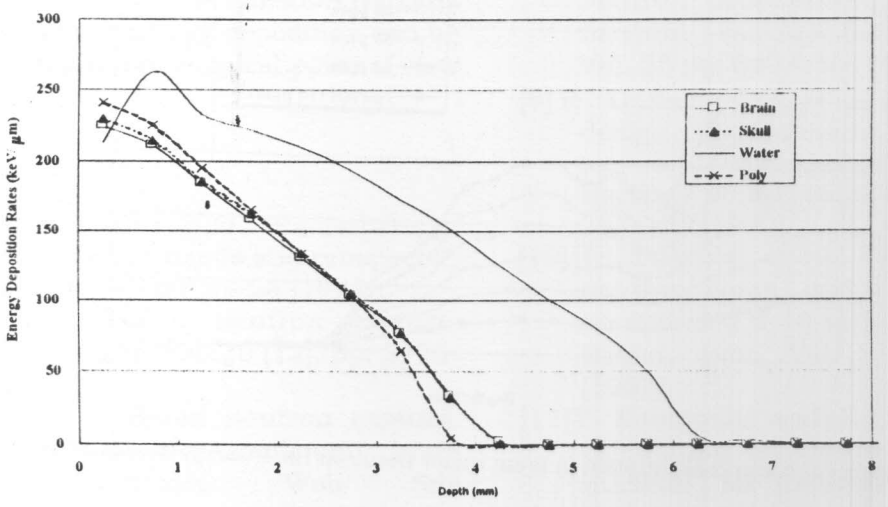

Fig. 7. Rate of energy deposition in different tissues due to lithium ions (keV/μm).

6.2. Comparison between energy deposition rates due to BNCT and nitrogen neutron capture (NNC) in brain tissues

Since it is critical for the successful application of the BNCT technique to have a BNCT dose in the tumor that is high compared to the dose to normal tissues, a comparison of the BNCT to NNC rate of energy deposition is needed. This should be done for different boron concentrations in brain tumor tissue as indicated in section 5.1. Results are shown in figs. 8 and 9. Notice that the boron concentration varies while the nitrogen concentration is constant. As mentioned in ref. 7, a 10 ppm of boron in normal healthy brain tissue is assumed for a boron concentration of 30 ppm in brain tumor tissue.

It is obvious from the figures that the relative energy deposition rate is quite remarkable especially in the first few microns due to Li compared with the He ions. Reference should be made to Fig.1 where the absolute values for the energy deposition rates of He, Li, and P in brain tissue are shown. figs. 8 and 9 can be used as rough evaluation for the different doses involved in the BNCT and to properly assess the dose to healthy tissue compared with the tumor tissue where the boron is concentrated.

7. Conclusions

1. Ranges and energy deposition rates for the proper branching ratios of the alpha, lithium, as well as protons can be properly simulated for the different phantoms used in the BNCT.
2. Ranges of alpha and lithium ions in brain and skull tissue are nearly the same. Thus, simulation of energy deposition in both tissues can use the same values for energy deposition rate.
3. Water phantoms tend to overestimate the ranges of alpha ions compared with the brain phantom.
4. For alpha ions, water phantom slightly underestimates the rate of energy deposition compared with brain phantoms especially below 6 microns. The reverse is observed after 6 microns where the water phantom slightly overestimates the rate of energy deposition.
5. There is a large overestimation of the energy deposition rate for lithium particles in water phantoms compared with brain phantoms.

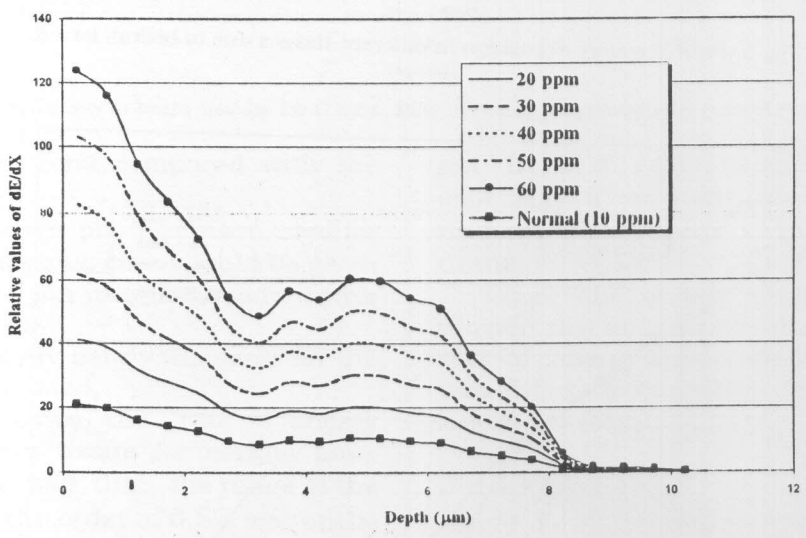

Fig. 8. Effect of boron concentration in brain tumor tissue on He/P energy deposition rates.

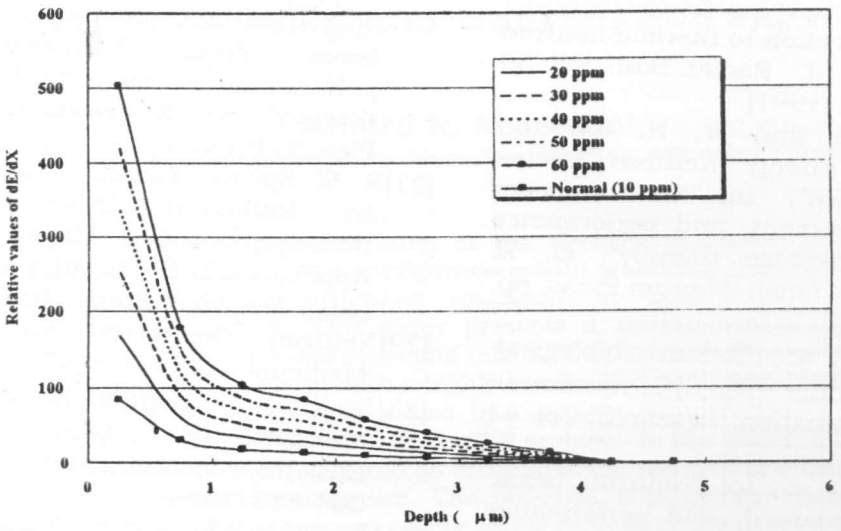

Fig. 9. Effect of boron concentration in brain tumor tissue on Li/P energy deposition rates.

6. He/P and Li/P energy deposition rates are quite remarkable especially in the first few microns due to Li compared with the He ions.
7. Evaluation for the different doses involved in the BNCT and assessment of the dose to healthy tissue compared with the tumor tissue where the boron is concentrated can be roughly estimated.
8. Regardless of the fact that the range of the carbon ions in brain tissue is of the order of 0.5 micron, their rate of energy deposition is relatively high. Thus, the BNCT/NNC ratio would be reduced at least in the first fractions of a micron. The question remains whether this rate of energy deposition can be neglected from a radiobiological point of view or not.

References

[1] F. A. Durosinmi-Etti, et al., "Radiotherapy in Africa: Current needs and prospects", IAEA Bulletin, (4), pp. 24-28 (1991).
[2] R. F. Barth, "Boron neutron capture therapy", Cancer, Vol. 70 (12), pp. 2995-007 (1992).
[3] J. G. Gomez, "Boron neutron capture therapy (BNCT) for malignant brain tumors", Internet Web Site www.virtualtrials.com,
[4] BNCT Briefing book, http//: www.id.inel.gov.
[5] Harvard Medical school home page on BNCT.
[6] R. M. Brugger, et al., in: "Neutron beam design, development, and performance for neutron capture therapy", O. K. Harling, et al., (eds), Plenum Press, pp. 3-12 (1990).
[7] M. Frederick Hawthorne, "From mummies to rockets and on to cancer therapy", Ineternet Web site web.chem.ucla.edu
[8] Y. Oka, et al., "A design study of the neutron irradiation facility for boron neutron capture therapy", Nuc. Tech., Vol. 55 pp. 642-655 (1981).
[9] R. G. Zamenhof, et al., in: "Neutron beam design, development, and performance for neutron capture therapy", O. K. Harling, et al., (eds), Plenum Press, pp. 283-305 (1990).
[10] H. Fukuda, et al., "RBE of a thermal neutron beam and the B(n,α)Li reaction on cultured B-16 melanoma cells", Int. J. Radiat. Biol., Vol. 51 (1), pp. 167-175 (1987).
[11] T. Kobayashi and K. Kanda, "Analytical calculation of Boron-10 dosage in cell nucleus for neutron capture therapy", Rad. Res., Vol. 91 pp. 77-94 (1982).

[12]D. E. Charlton, "Energy deposition in small ellipsoidal volumes by high-LET particles: application to thermal neutron dosimetry", Int. J. Radiat. Biol., Vol. 59 (3), pp. 827-842 (1991).

[13]R. M. Brugger and W. H. Herleth, "Intermediate Energy Neutron Beams from the MURR", in: "Neutron beam design, development, and performance for neutron capture therapy", O. K. Harling, et al., (eds), Plenum Press, pp. 153-166 (1990).

[14]M. A. Davis, et al., "Relative biological effectiveness of the $^{10}B(n,\alpha)^{7}Li$ reaction in Hela cells", Radiation Research, Vol. 43 534553 (1970).

[15]J. R. Choi, et al., in: "Neutron beam design, development, and performance for neutron capture therapy", O. K. Harling, et al., (eds), Plenum Press, pp. 201-218 (1990).

[16]E. Grusell, et al., "The Possible Use of a Spallation Neutron Source for Neutron Capture Therapy with Epithermal Neutrons", in: "Neutron beam design, development, and performance for neutron capture therapy", O. K. Harling, et al., (eds), Plenum Press, pp. 349-358 (1990).

[17]H. Madoc-Jones, et al., in: "Neutron beam design, development, and performance for neutron capture therapy", O. K. Harling, et al., (eds), Plenum Press, pp. 23-35 (1990).

[18]R. Gahbauer, et al., "BNCT: a promising area of research?", http//: www-radonc.med.ohio-state.edu.

[19]J. G. Gomez, "Boron neutron capture therapy (BNCT) for malignant brain tumors", Internet Web Site www.virtualtrials.com.

[20]F. J. Wheeler et al., "Physics design for the Brookhaven medical research reactor epithermal neutron source", in: "Neutron beam design, development, and performance for neutron capture therapy", O. K. Harling, et al., (eds), Plenum Press, pp. 83-95 (1990).

[21]F. W. Spiers, Transition-Zone Dosimetry, in: Radiation Dosimetry, Vol. III, Sources, Fields, Measurements, and Applications, F. H. Attix and E. Tochilin (eds), Academic Press, (1969).

[22]Neutron Dosimetry for Biology and Medicine, ICRU 26, (1977).

[23]K. Kitao, "A method for calculating the absorbed dose near interface from $B(n,\alpha)Li$ reaction, Read. Res., Vol. 61 pp. 304-315 (1975).

[24]T. Kobayashi and K. Kanda, "Analytical calculation of Boron-10 dosage in cell nucleus for neutron capture therapy", Rad. Res., Vol. 91 pp. 77-94 (1982).

[25]D. Gabel, et al., "The Monte Carlo simulation of the biological effect of the $^{10}B(n,\alpha)^{7}Li$ reaction in cells and tissue and its implication for boron neutron capture therapy", Rad. Res., Vol. 111 pp. 14-25 (1987).

[26]H. Fukuda, et al., "RBE of a thermal neutron beam and the $^{10}B(n,\alpha)^{7}Li$ reaction on cultured B-10 melanoma cells", Int. J. Radiat. Biol., Vol. 51 pp. 167-175 (1987).

[27]S. Han, "Computer Simulation Of Ion Beam Mixing", Ph.D. Thesis, University of Wisconsin-Madison, USA, (1988).

Received May 7, 2000
Accepted January 15, 2001